

Modifying the buried interface with azodicarbonamide for high-efficiency MA-free perovskite solar cells

Jin Kang^a, Huan Bi^{b}, Mengna Guo^c, Yao Guo^d, Hanjun Zou^e, Gaoyi Han^{c*}, and
Wenjing Hou^{c*}*

^a Department of Chemistry and Chemical Engineering, Collaborative Innovation Center for Functional Chemicals, High Value Fine Chemicals Research Center, Jinzhong University, Jinzhong, 030619, Shanxi China.

^b Faculty of Informatics and Engineering, The University of Electro-Communications, 1-5-1 Chofugaoka, Chofu, Tokyo 182-8585, Japan.

^c Institute of Molecular Science, Key Laboratory of Materials for Energy Conversion and Storage of Shanxi Province, Shanxi University, Taiyuan 030006, P. R. China

^d School of Materials Science and Engineering, Henan Joint International Research Laboratory of Nanocomposite Sensing Materials, Anyang Institute of Technology, Anyang 455000, China

^e Analytical and Testing Center, Chongqing University, Chongqing 401331, China

*Corresponding Author (H. Bi, G.Y. Han, W.J. Hou)

E-mail: hbi.trans.sci@uec.ac.jp

E-mail: han_gaoyis@sxu.edu.cn

E-mail: houwenjing@sxu.edu.cn

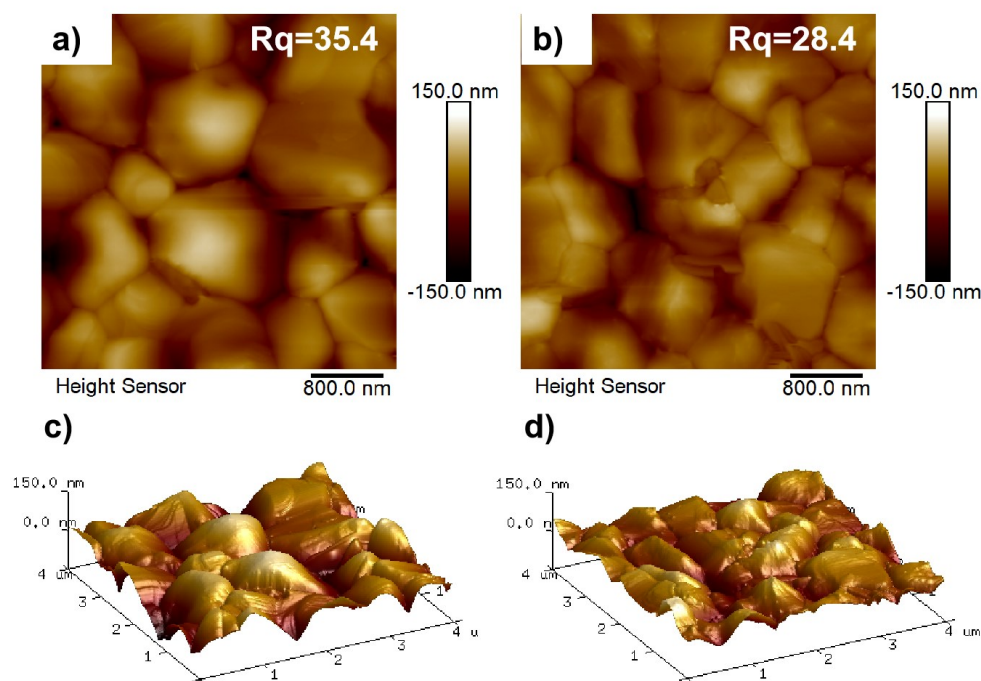


Fig. S1. Two- and three- dimensional AFM images of perovskite films spin-coated on (a,c) the TiO_2 and (b,d) ADC-modified TiO_2 substrates.

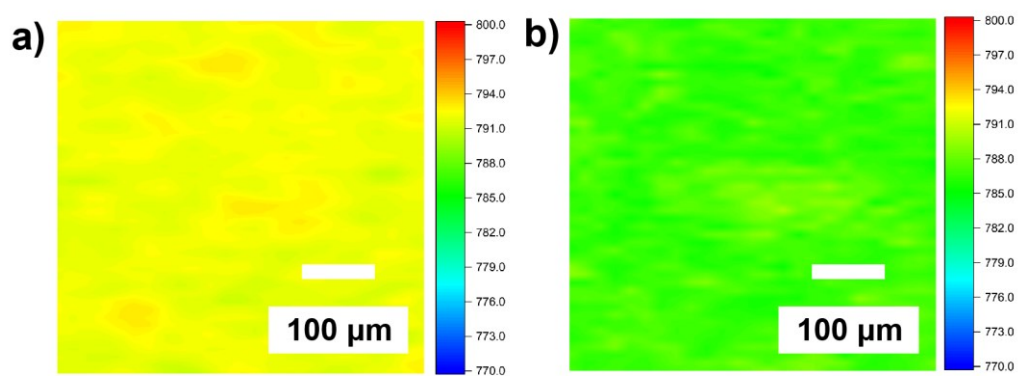


Fig. S2. PL position mapping images of the (a) control and (b) target perovskite film.

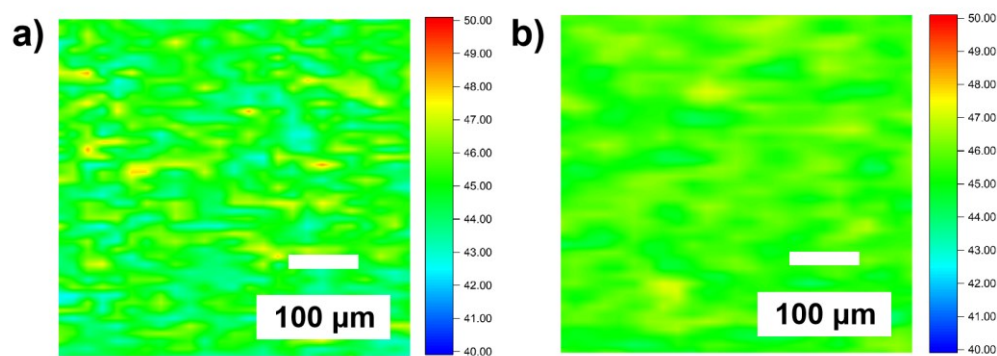


Fig. S3. PL full width at half maxima of the (a) control and (b) target perovskite film.

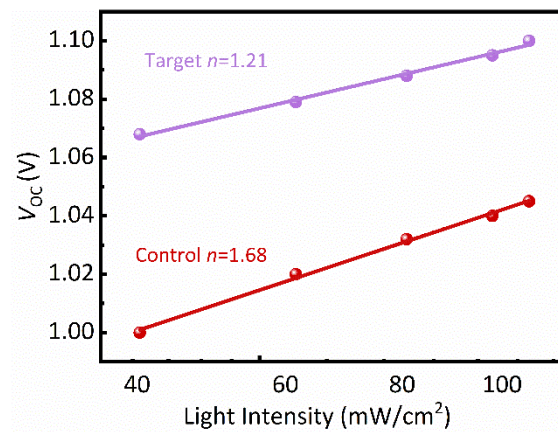


Fig. S4. V_{OC} versus light intensity for the control and target devices.

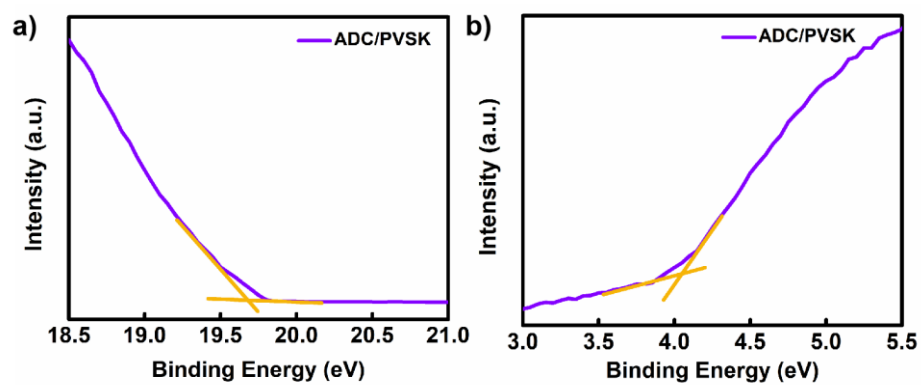


Fig. S5. UPS spectra of ADC/PVSK: (a) secondary electron cutoff regions, and (b) Fermi edge region.

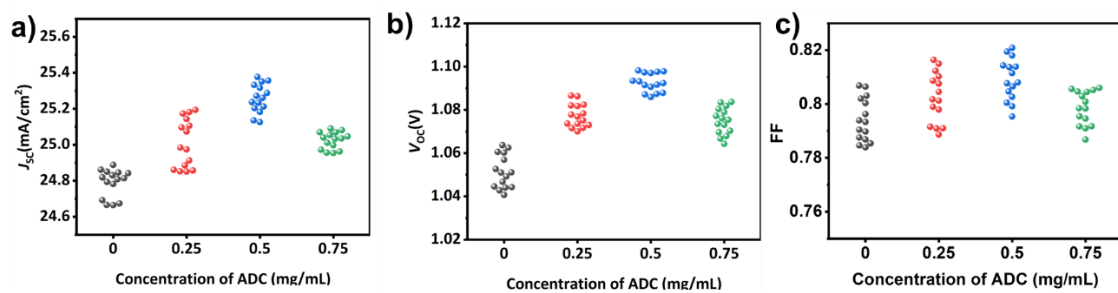


Fig. S6. Statistics of (a) J_{SC} , (b) V_{OC} , and (c) FF of PSCs based on TiO_2 modified by different concentrations of ADC.

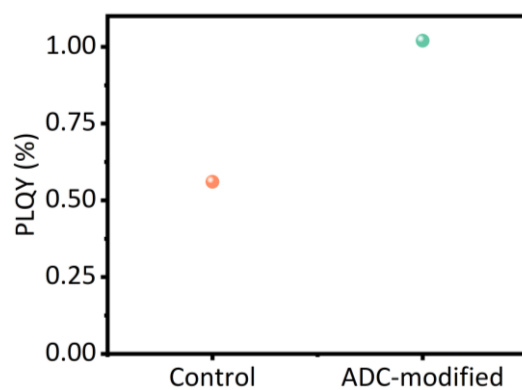


Fig. S7. PLQY for the layer structure glass/FTO/TiO₂/(without or with ADC)/perovskite.

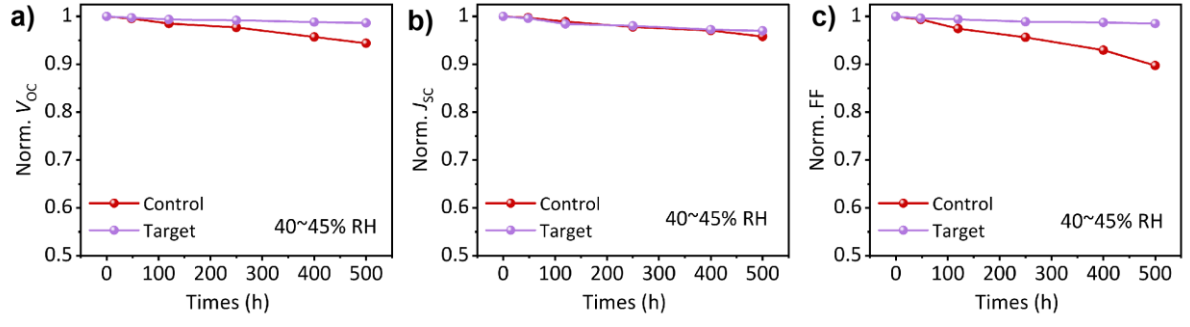


Fig. S8. (a) V_{OC} , (b) J_{SC} , and (c) FF as a function of time for the unencapsulated control and target devices aged under a relative humidity of 40-45% at room temperature in the dark.

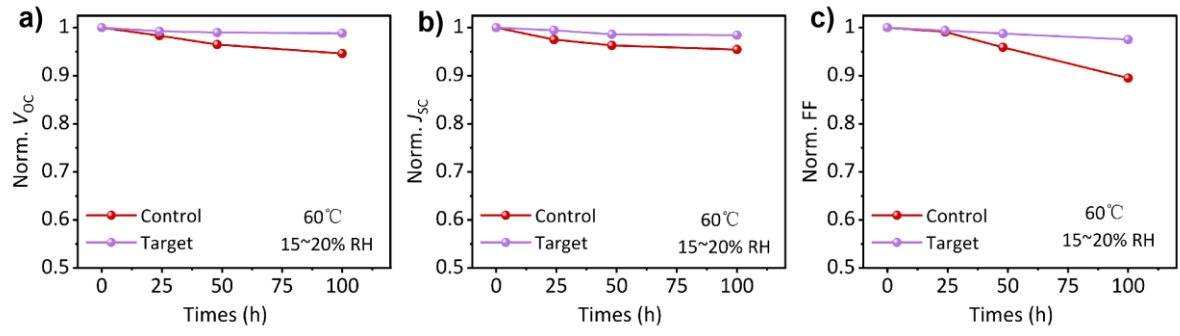


Fig. S9. (a) V_{OC} , (b) J_{SC} , and (c) FF as a function of time for the unencapsulated control and target devices aged at 60 °C in the dark where the unencapsulated devices were located in the air condition.

Table S1 Fitted results of TRPL curves of the perovskite films deposited on the glass or with glass+ADC.

| | Glass/PVSK | Glass/ADC/PVSK |
|-------------------|------------|----------------|
| τ_1 (ns) | 23.88 | 18.17 |
| % | 60.2 | 45.5 |
| τ_2 (ns) | 107.63 | 110.84 |
| % | 39.8 | 54.5 |
| τ_{ave} (ns) | 86.57 | 99.68 |

Table S2 Fitted results of TRPL curves of the perovskite films deposited on the substrates with TiO_2 or with TiO_2+ADC .

| | FTO/ TiO_2 /PVSK | FTO/ TiO_2 /ADC/PVSK/ |
|--------------------------|---------------------------|--------------------------------|
| τ_1 (ns) | 5.47 | 4.40 |
| % | 76.8 | 84.4 |
| τ_2 (ns) | 23.79 | 19.61 |
| % | 23.2 | 15.6 |
| τ_{ave} (ns) | 15.85 | 11.27 |

Table S3. Photovoltaic parameters of the PSCs based on TiO₂ modified with different concentrations of ADC from 0 to 0.75 mg/mL.

| ADC (mg/mL) | Samples | J_{sc} (mA/cm ²) | V_{oc} (V) | FF | PCE (%) |
|----------------|----------|-----------------------------------|-----------------|-------------|-------------|
| 0 | Champion | 24.67 | 1.047 | 0.806 | 20.82 |
| | Average | 24.78±0.099 | 1.051±0.012 | 0.793±0.013 | 20.69±0.146 |
| 0.25 | Champion | 25.01 | 1.077 | 0.803 | 21.61 |
| | Average | 25.19±0.184 | 1.086±0.009 | 0.816±0.134 | 21.79±0.171 |
| 0.5 | Champion | 25.38 | 1.098 | 0.820 | 22.52 |
| | Average | 25.25±0.118 | 1.092±0.005 | 0.809±0.117 | 22.32±0.196 |
| 0.75 | Champion | 25.09 | 1.084 | 0.805 | 21.69 |